

## 22nm Node p+ Junction Scaling Using B<sub>36</sub>H<sub>44</sub> And Laser Annealing With or W/O PAI

John Borland<sup>1</sup>, Masayasu Tanjyo<sup>2</sup>, Nariaki Hamamoto<sup>2</sup>, Tsutomu Nagayama<sup>2</sup>, Shankar Muthukrishnan<sup>3</sup>, Jeremy Zelenko<sup>3</sup>, Iad Mirshad<sup>4</sup>, Walt Johnson<sup>4</sup> and Temel Buyuklimanli<sup>5</sup>

- 1) J.O.B. Technologies, Aiea, Hawaii, 96701
- 2) Nissin Ion Equipment, Kyoto, Japan
- 3) Applied Materials, Sunnyvale, CA
- 4) KLA-Tencor, San Jose, CA
- 5) EAG, East Windsor, NJ

**Abstract**-B<sub>36</sub>H<sub>44</sub> molecular dopants were implanted at 100eV and 1E15/cm<sup>2</sup> B equivalent energy and dose to achieve Xj<7nm and selected wafers also had various PAI (pre-amorphizing implantation) using Ge 10keV, Xe 14keV and In 14keV to create an amorphous layer 16-17nm deep. All the wafers were MSA (msec annealed) by DSA laser at 1175°C, 1225°C, 1275°C and 1325°C and the results show that the Rs and Bss values for B<sub>36</sub>H<sub>44</sub> without PAI was always better than those reported using monomer B and BF<sub>2</sub> with MSA even though the retained dose was only 67% compared to 100% for monomer B and 55% for BF<sub>2</sub> and we noted that the surface oxide directly affects the retained dose. Adding Ge or In PAI had no effect on dopant activation due to the self-amorphization effects of B<sub>36</sub>H<sub>44</sub> however, Xe-PAI improved activation by 20% but degraded junction leakage. In-PAI also had the highest lifetime. However, we noted that Xe-PAI behaves differently compared to Ge-PAI and In-PAI, TW values were always much higher and independent of the anneal technique (MSA, spike/RTA or furnace anneal) even though no defects could be detected by X-TEM suggesting uniform distribution of vacancy cluster defects throughout the amorphous region.

### INTRODUCTION

For the 22nm node bulk planar CMOS will still be used with targeted p+ Xj between 6-12nm and FinFET CMOS devices delayed until the 16nm node. Using monomer B beam-line implantation Borland et al. [1] reported this would require energies as low as 83eV and the concern of severe energy contamination for productivity decel ratio implant conditions of >50/1. Using BF<sub>2</sub> increases the implant energy to about 500eV but at these shallow depths only about 55% of the implanted B dose is retained in the silicon wafer and 50% of this dose is in the surface native oxide which can vary between 1.1-2.3nm and grow during implantation [2]. To enhance dopant activation with MSA only annealing a PAI implant is needed for B and BF<sub>2</sub> but not with molecular dopants as reported by Borland et al. [2,3] and PAI can lead to residual EOR damage and junction leakage degradation. Therefore we decided to investigate the use of boron molecular dopants as an alternative to using B or BF<sub>2</sub>. B<sub>18</sub>H<sub>22</sub> (B<sub>18</sub>) had been widely studied down to 200eV equivalent B energies so we selected B<sub>36</sub>H<sub>44</sub> (B<sub>36</sub>) for 100eV equivalent energies as 1<sup>st</sup> reported by Tanjyo et al. [4].

### EXPERIMENTATION

The Nissin Claris cluster-B implanter was used for the B<sub>36</sub> implantation and the Applied Materials DSA laser annealer was used to anneal selected regions on 300mm n-type wafers at 1175°C, 1225°C, 1275°C and 1325°C as shown below in Fig. 1. Additionally some wafers received different PAI implant species, Ge-PAI, Xe-PAI or In-PAI. To evaluate the effects of PAI+B<sub>36</sub> on enhanced dopant activation as previously reported for monomer B and BF<sub>2</sub> [2] and residual implant damage and EOR defects some wafers had 10keV Ge-PAI at 1 or 5E14/cm<sup>2</sup>, 14keV Xe-PAI at 1 or 0.5E14/cm<sup>2</sup> and 14keV In-PAI at 1 or 0.5E14/cm<sup>2</sup>.

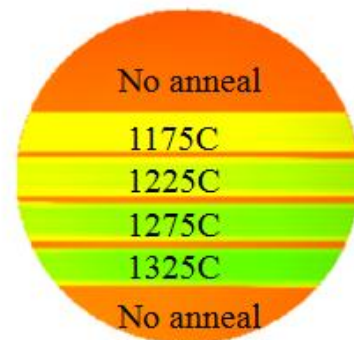


Fig.1: Thermal-wave full wafer image mapping showing the 4 different laser annealing temperature zones created by the DSA laser scan.

### RESULTS

Evans Analytical Group (EAG) measured the B<sub>36</sub>, Xe-PAI, In-PAI and surface native oxide shallow surface depth profile using their special high depth resolution PCOR-SIMS technique. This allowed the determination of both the physical and the electrical junction depth (Xj) profiles including surface oxide thickness. Sheet resistance (Rs) was measured by 4PP at KLA-Tencor (KT) using their flat Hx-probes and by RsL at Frontier Semiconductor (FSM). Plotting Rs versus Xj we then determined the electrical dopant activation level Bss (boron solid solubility). Residual implant damage and EOR defects were measured by X-TEM, thermal-wave (TW) and Quantox lifetime at KT and RsL junction leakage current at FSM.

#### Dopant Profile & Activation Analysis

High depth resolution (HDR) PCOR-SIMS B<sub>36</sub> dopant profile for as-implanted no anneal region and 1325°C

DSA laser anneal region is shown in Fig.2. The physical B junction depth is 8.2nm as implanted and 8.8nm after anneal but the surface native oxide thickness was determined to be 1.1nm thick by PCOR-SIMS so the corrected electrical junction depth  $X_j$  was determined to be 7.1nm and 7.7nm respectively and labeled in Fig.2.  $R_s$  measured by 4PP was 1522 ohms/sq and 1520 ohms/sq by RsL so the calculated dopant activation  $B_{ss}$  value of  $1.2E20/cm^3$  is shown in the  $R_s$  versus  $X_j$  chart of Fig. 3. The B retained dose was  $7.7E14/cm^2$  for as-implanted and  $6.6E14/cm^2$  after anneal for a dose loss of  $1.1E14/cm^2$ . With Ge, Xe or In PAI the as-implanted B depth profiles were identical as shown in Fig.4 with the corrected electrical  $X_j=6.6nm$  since these wafers had a thicker 1.6nm surface oxide and retained dose of  $6.7E14/cm^2$ . Note that the PAI implantation results in an additional 0.5nm of surface oxide growth compared to no PAI wafer and there was no additional oxide growth from the DSA laser annealing process. Fig.5 shows the relationship of  $B_{36}$  retained dose in the wafer versus surface oxide thickness suggesting that we need zero surface oxide to achieve 100%  $B_{36}$  retained dose. In Fig.2 without PAI we observed 0.6nm of diffusion with  $B_{36}$  only while with PAI we observed significant amount of B diffusion/movement (TED). With Xe-PAI TED was 3.4nm, with In-PAI TED was 3.6nm and with Ge-PAI TED was 4.7nm. The retained dose after anneal dropped to  $6.5E14/cm^2$  (loss of  $2E13/cm^2$  dose).  $R_s$  values for Ge-PAI was 1204 ohms/sq by 4PP and 1256 ohms/sq by RsL, for In-PAI it was 1218 ohms/sq by 4PP and 1290 ohms/sq by RsL, and for Xe-PAI only RsL gave a value of 834 ohms/sq. This corresponds to a dopant activation  $B_{ss}$  level of  $1.1E20/cm^3$  for both the Ge-PAI and In-PAI while for Xe-PAI  $B_{ss}=1.5E20/cm^3$  as shown in Fig.3. To further reduce residual implant damage and EOR defects a  $900^\circ C$  spike/RTA diffusion-less anneal before the DSA laser anneal was done for the Xe-PAI and In-PAI samples as shown in Figs. 4 & 6. We observed about 0.3nm of additional surface oxide growth from the  $900^\circ C$  spike/RTA anneal as detected by PCOR-SIMS resulting in 1.8-1.9nm total surface oxide. The retained dose after spike/RTA was  $6.8E14/cm^2$  and TED for the Xe-PAI was 6.2nm compared to only 5.0nm for the In-PAI samples. After the additional  $1325^\circ C$  laser anneal 1.3nm of additional B movement was detected for the Xe-PAI case while no additional change in  $X_j$  with In-PAI however, there was noticeable B dopant motion in the  $E19/cm^3$  level resulting in a more abrupt profile in Fig. 7 of 2.1nm/decade versus 3.8nm/decade and we have no explanation for this. We examined the In-PAI In dopant profile in more detail as shown in Fig. 8. Note that the as-implanted In peak ( $R_p$ ) was  $9E19/cm^3$  at 13nm depth but after each anneal this level drops to  $<4E18/cm^3$  and the chemical In dopant piles-up at the surface interface to a level  $>2E20/cm^3$ . Xe on the other hand diffuses out of the silicon surface as shown in Fig.9 where the as-implanted Xe peak ( $R_p$ ) was  $8E19/cm^3$  at a depth of 13nm and after the  $1325^\circ C$  anneal the Xe level drops to below the SIMS background detection limit of  $<1E19/cm^3$ .

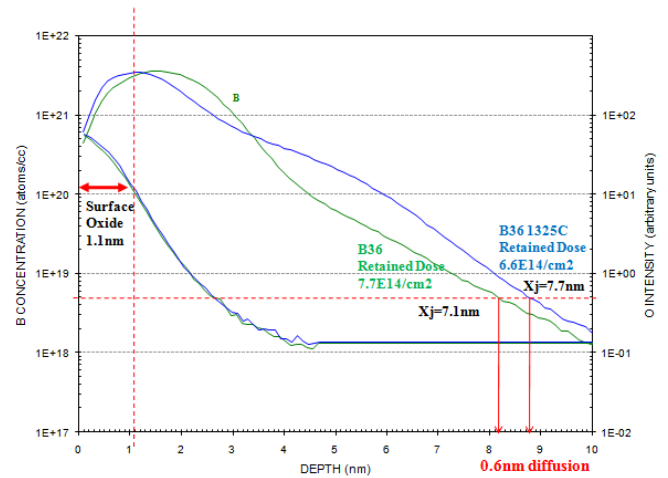


Fig.2: B36 PCOR-SIMS results for as-implanted and after  $1325^\circ C$  laser anneal.

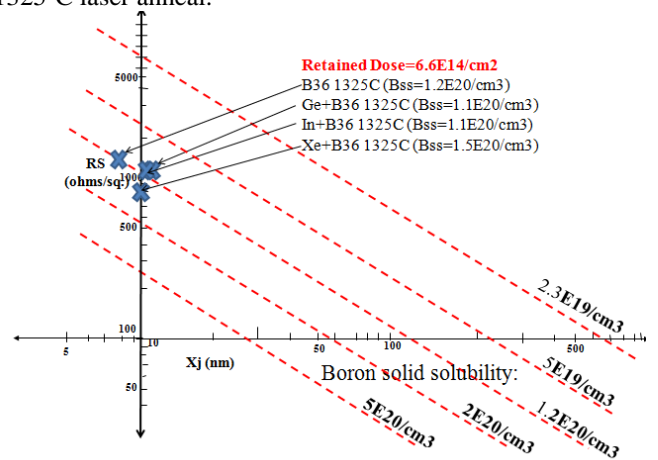


Fig.3:  $R_s$  versus  $X_j$  chart for  $B_{36}$  with and w/o PAI.

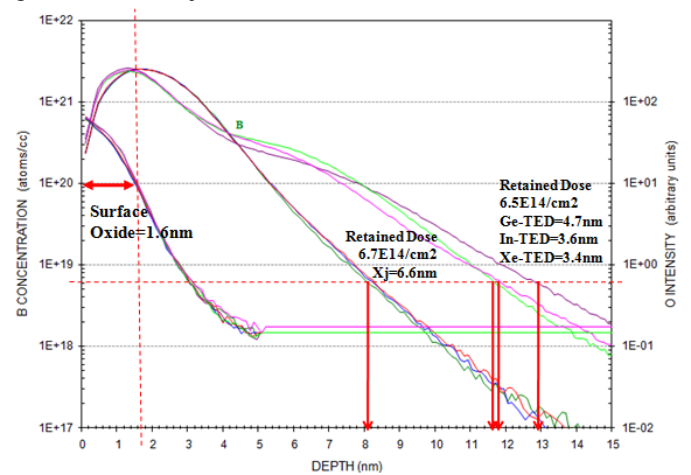


Fig.4: PCOR-SIMS results for  $B_{36}$  with Ge, Xe and In PAI.

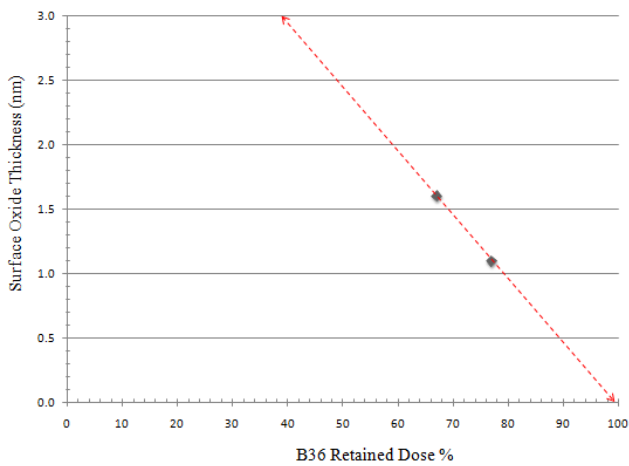


Fig.5: B<sub>36</sub> retained dose in the wafer versus surface oxide thickness.

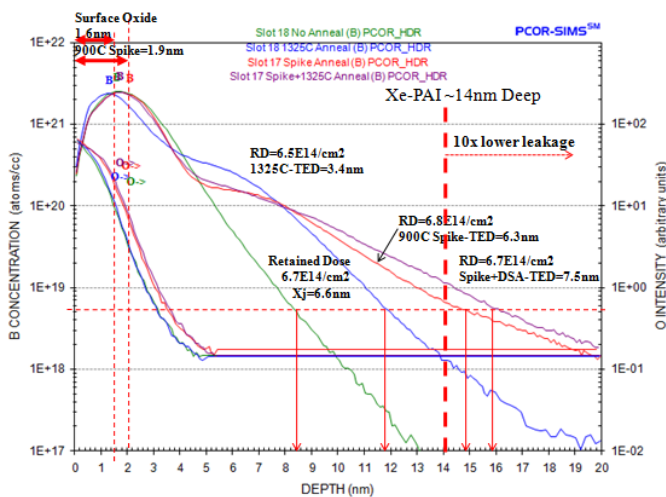


Fig.6: PCOR-SIMS results for Xe-PAI+B<sub>36</sub> no anneal, 1325°C laser, 900°C spike/RTA and 900°C spike/RTA+1325°C laser.

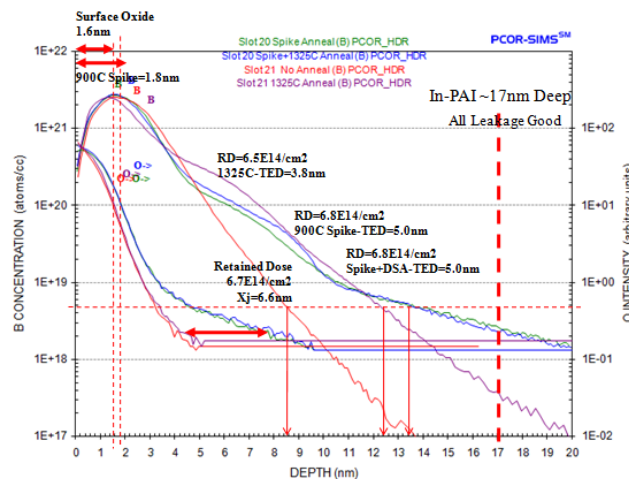


Fig.7: PCOR-SIMS results for In-PAI+B<sub>36</sub> no anneal, 1325°C laser, 900°C spike/RTA and 900°C spike/RTA+1325°C laser.

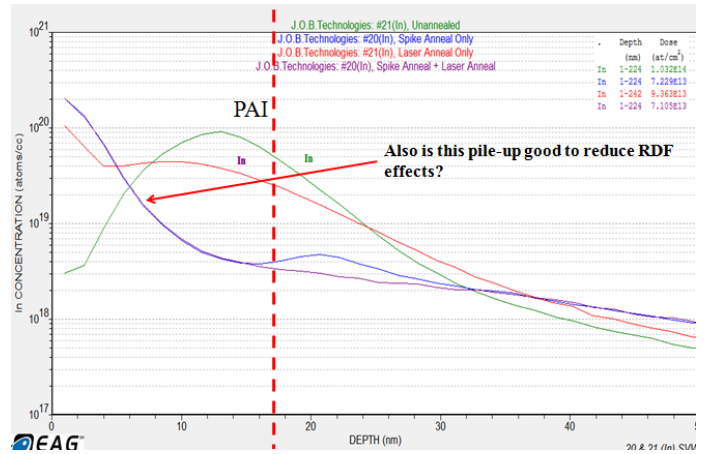


Fig.8: PCOR-SIMS results for In-PAI no anneal, 1325°C laser, 900°C spike/RTA and 900°C spike/RTA+1325°C laser.

### Xe-PAI No Anneal & 1325C Anneal

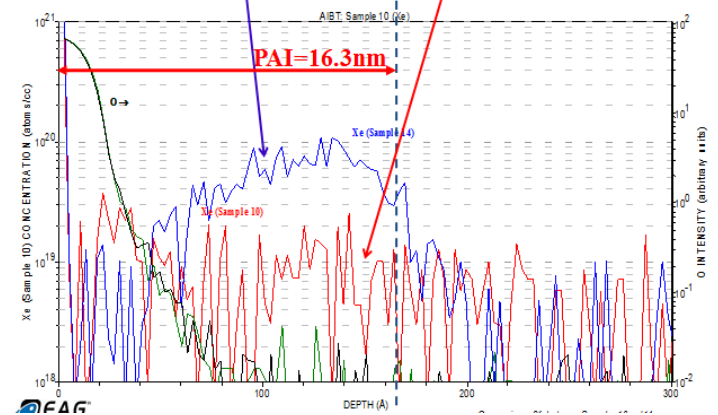


Fig.9: PCOR-SIMS results for Xe-PAI no anneal and 1325°C laser.

### Defect Analysis

X-TEM results for Xe-PAI and In-PAI are shown in Figs. 10 & 11 respectively for the no anneal and 1325°C anneal regions. The 14keV Xe-PAI implant results in a 16.3nm deep amorphous layer while the 14keV In-PAI implant amorphous layer is 17nm deep. After the 1325°C laser anneal no evidence of residual implant damage nor EOR defects could be observed for either the Xe-PAI nor the In-PAI wafers. However, both RsL junction leakage results in Fig. 12 and TW results in Fig. 1 did detected Xe residual implant damage not visible by X-TEM and these defects are not the usual EOR damage beyond the amorphous layer observed with Ge-PAI. The RsL junction leakage current results in Fig. 12 shows that the Ge-PAI junction leakage improved by over an order of magnitude for each higher peak temperature laser anneal going from 9.1E-5A/cm<sup>2</sup> at 1175°C to 4.9E-6A/cm<sup>2</sup> at 1225°C to 1.0E-7A/cm<sup>2</sup> at 1275°C and finally to <5E-8A/cm<sup>2</sup> at 1325°C. This trend is similar to TW which goes from 14,052 no anneal to 2,558 at 1175°C to 2,213 at 1225°C to 1,837 at 1275°C and finally to 1,715 at 1325°C in Fig.13. What was confusing at first was the Xe-

PAI results with higher annealing peak temperature had no effect on improving junction leakage current and reducing TW value suggesting the Xe residual implant damage was very stable and would not anneal out possibly vacancy clusters as reported by Salnik et al. [8]. Note that RsL leakage level was upper E-4 to lower E-3A/cm<sup>2</sup> but the additional 900°C Spike/RTA anneal step did reduce the leakage level by up to 100x to upper E-6A/cm<sup>2</sup> due to 3.7nm deeper junction as shown by the B depth profile in Fig. 6 but this additional spike anneal had no effect in reducing the TW value suggesting no defect reduction only junction diffusion (deeper junction). Also note that the In-PAI wafers had the lowest RsL junction leakage current all below the lower detection limit of <5E-8A/cm<sup>2</sup> irrespective of annealing temperature. The In-PAI TW values were also very low as shown in Fig.13. To further characterize the difference in defect levels between Xe-PAI and In-PAI we used the KT Quantox system to measure minority carrier lifetime and the results are shown in Fig.14. To our surprise the In-PAI wafers after anneal had the highest surface lifetimes suggesting very high quality silicon free of defects. In is a group III element and know to be gettered by defects which caould explain the low junction leakage and high lifetimes. Xe-PAI wafers had low lifetimes again independent of peak laser annealing temperature. The Ge-PAI wafers lifetime increased with increasing laser peak temperature.

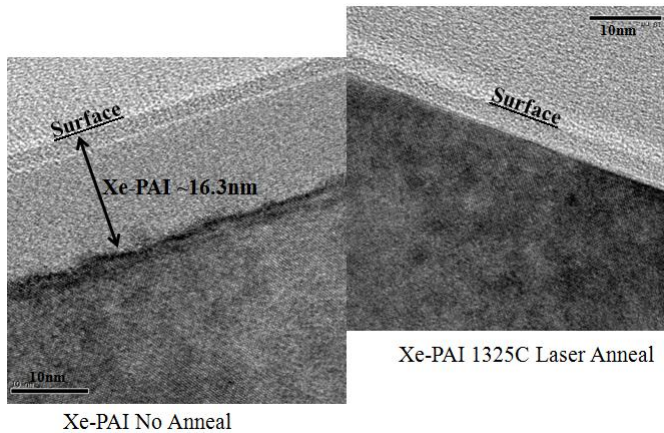


Fig.10: X-TEM analysis of Xe-PAI before and after 1325°C laser anneal.

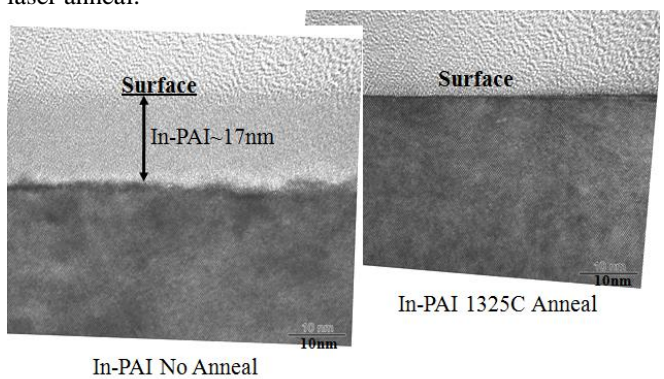


Fig.11: X-TEM analysis of In-PAI before and after 1325°C laser anneal.

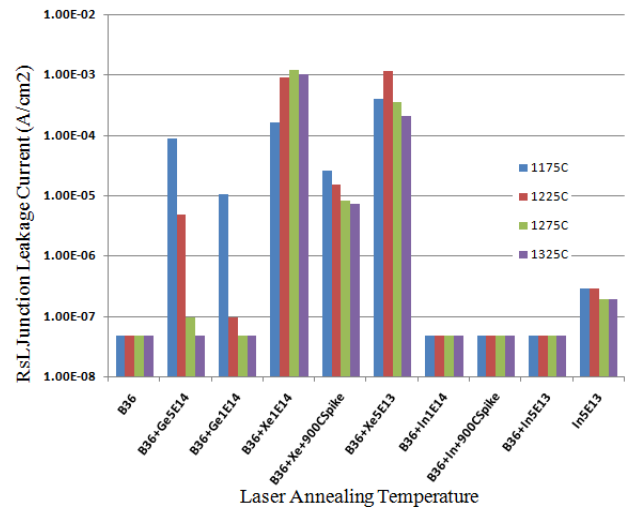


Fig.12: Effects of implant and annealing conditions on junction leakage current.

### B36 TW Results

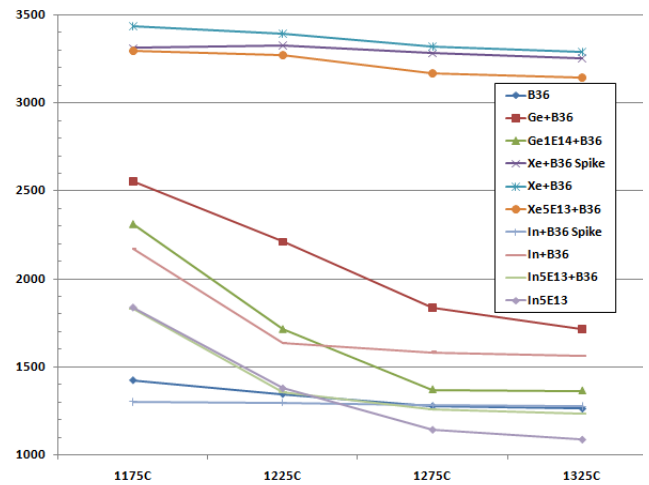


Fig.13: Residual implant damage detected by thermal-wave analysis.

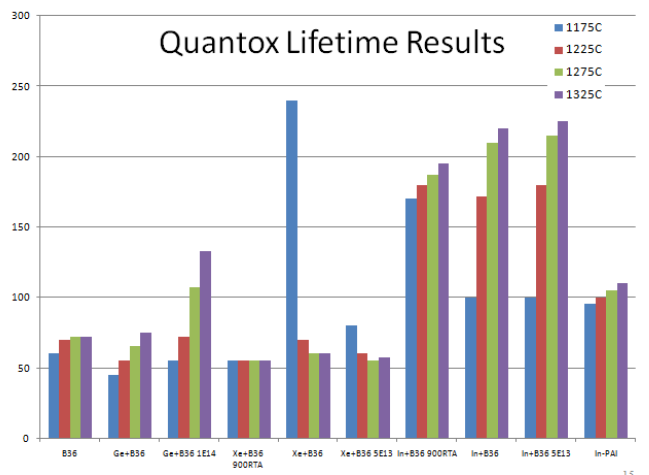


Fig.14: Comparison of minority carrier lifetime results to implant and annealing conditions and surface defect level.

## SUMMARY

$B_{36}$  molecular dopant implantation at  $100\text{eV}/1\text{E}15/\text{cm}^2$  B equivalence resulted in as-implanted junction depths  $<7\text{nm}$  targeting the  $22\text{nm}$  node. Increasing DSA laser annealing peak temperatures from  $1175^\circ\text{C}$  up to  $1325^\circ\text{C}$  improved dopant activation. Only  $0.6\text{nm}$  of dopant diffusion was observed when using only B36 with self-amorphization and a dopant activation Bss value of  $1.2\text{E}20/\text{cm}^3$  was achieved. With Ge-PAI,  $4.7\text{nm}$  of dopant movement (TED) was observed with no improvement in dopant activation (Bss= $1.1\text{E}20/\text{cm}^3$ ) but degradation in junction leakage current for lower annealing temperatures. In-PAI resulted in  $3.6\text{nm}$  of TED, Bss= $1.1\text{E}20/\text{cm}^3$  and best surface lifetime and low junction leakage for all the annealing temperatures. Xe-PAI had the best dopant activation (Bss= $1.5\text{E}20/\text{cm}^3$ ) but resulted in high TW values believed to be due to vacancy cluster defects degrading junction leakage current and surface lifetime but a  $900^\circ\text{C}$  spike/RTA anneal results in  $3.7\text{nm}$  of B diffusion thereby improving junction leakage current by  $>100\text{x}$ . Higher dopant activation Bss values will require higher implantation doses possibly  $>3\text{E}15/\text{cm}^2$  with even thinner surface native surface oxide of  $<0.5\text{nm}$  to achieve higher B retained dose.

## ACKNOWLEDGMENTS

The authors are grateful to Yuen Lim of Frontier Semiconductor for support with RsL leakage and Rs measurements.

## REFERENCES

- 1] J. Borland, S. Felch, Z. Wan, M. Tanjyo and T. Buyuklimanli, Solid State Technology, August 2009, p.14.
- 2] J. Borland, Z. Wan, S. Muthukrishnan, J. Zelenko, I. Marshid, W. Johnson and T. Buyuklimanli, Insights-2009 meeting April 26-29, 2009, Napa,CA, p.25.
- 3] J. Borland, Y. Kawasaki, J. Halim and B. Chung, Solid State Technology, July 2008, p.38.
- 4] M. Tanjyo, N. Hamamoto, T. Nagayama, S. Umisedo, Y. Koga, N. Maehara, H. Ume, T. Matsumoto, N. Nagai and J. Borland, Semicon/China 2009, ISTC/CSTIC 2009, China Semiconductor Technology International Conference, March 19-20, 2009, Shanghai, China, p.234.
- 5] A. Salnik et al., Semicon/West 2009 WCJUG meeting presentation material, July 16, 2009.